

# Appendix E

## Intruder Probabilistic Models

### E.1 Linear Intersection

**Idea:** There are *small intruders* which have body *smaller* than average  $cell_{i,j,k}$  cell size. Its trajectory will stick to *linear trajectory* prediction with high probability.

**Space Intersection Rate:** The *Space Intersection Rate* for  $cell_{i,j,k}$  is implemented as simple point cloud intersection. Where *sufficiently thick* point cloud is defined along *line* (eq. E.1):

$$position(time) = position(time_0) + velocity \times time, \quad time \in [0, \infty[ \quad (E.1)$$

Then there exist projection function from local Euclidean coordinates to local polar coordinates (eq. E.2). The function projects intruder trajectory (eq. E.1) to planar coordinates  $[distance, horizontal^\circ, vertical^\circ]$  as a set of sufficiently thick point cloud.

$$polarSet : position(t) \rightarrow \{[distance, horizontal^\circ], vertical^\circ\} \quad (E.2)$$

The *space intersection rating*  $SpaceIntersection(\circ)$  for line type is given as (eq. E.3). If there exist non empty intersection of  $polarSet \cap cell_{i,j,k}$  there is space intersection rate equal to 1, if intersection  $polarSet \cap cell_{i,j,k} = \emptyset$  then the rate is zero.

$$space \left( \begin{matrix} Intruder, \\ cell_{i,j,k} \end{matrix} \right) = \begin{cases} 1 : & \exists point \in polarSet(eq.E.2) : point \in c_{i,j,k} \\ 0 : & \text{otherwise} \end{cases} \quad (E.3)$$

*Note.* The *intruder intersection rate* is multiplication of *space intersection rate* and time intersection rate. The *intersection rate* is calculated for *every intruder* and *selected intersection model* separately.

## E.2 Body-volume Intersection

**Idea:** The *Intruder* has body volume greater than *average cell*<sub>*i,j,k*</sub> volume. The *intruder body* is considered as the ball moving along *intruder position*. The *intersection* of the intruder body is realized as sufficiently thick *point-cloud intersection*.

**Space Intersection Rate - Body Volume:** The *body volume mass* with center at *position*(*t*) is moving along intruder trajectory prediction (eq. E.4) in time interval  $[0, \infty[$ :

$$position(time) = position(time_0) + velocity \times time \quad (E.4)$$

The body *Volume ball* *Body*(*position*(*t*), *radius*) (eq. E.5) is defined as set of points in  $\mathbb{R}^3$  euclidean space. The center is moving along the *position*(*t*). The body *volume ball* is a set of points sufficiently thick including also inner points. The *thickness* is guaranteed by existence of neighbour point which is close enough.

$$Body(position(t), radius) = \left\{ \begin{array}{l} \|position(t) - point\| \leq radius \\ point \in \mathbb{R}^3 : \forall point_i \exists point_{j \neq i}, \\ distance(point_i, point_j) \leq thickness \end{array} \right\} \quad (E.5)$$

The *polar volume ball* *polarBody* (eq. E.6) is projection of body volume ball set *Body*(*position*(*t*), *radius*) to a set of planar coordinates in avoidance grid coordinate frame:

$$polarBall(t) : Body(position(t), radius) \rightarrow \left\{ \left[ \begin{array}{l} distance, horizontal^\circ, \\ vertical^\circ, intersectionTime \end{array} \right] \right\} \quad (E.6)$$

The *space intersection rate for vehicle body* *space*(*Intruder*, *cell*<sub>*i,j,k*</sub>) (eq. E.7) is calculated as intersection of polar body volume ball and *cell*<sub>*i,j,k*</sub>. If intersection is non empty then base probability is one, zero otherwise:

$$space \left( \begin{array}{l} Intruder, \\ cell_{i,j,k} \end{array} \right) = \begin{cases} 1 : & \exists point \in polarBall(eq.E.6) : point \in c_{i,j,k} \\ 0 : & \text{otherwise} \end{cases} \quad (E.7)$$

**Intersection Time:** The *intersection time* id depending on point cloud (eq. E.6) where each point *have intersection time* given as *body-center position* time (eq. E.4).

*Note.* The *body-volume* intersection model can insert the *multiple intersection times* into one *cell*<sub>*i,j,k*</sub>. The *interval length* considers all of these for intersection rates (eq. ??).

## E.3 Maneuverability Uncertainty Intersection

**Idea:** The *intruders* are not bullets they are not sticking to predicted linear paths. The *intruder* maneuverability is given as horizontal and vertical spread. Therefore *intruder reach set* will form an *elliptic cone*. This cone can be transformed into *finite discrete* point-cloud, each *point* should have assigned *severity* impact value. The point cloud intersection with *Avoidance Grid* will give us space impact of an *uncertain* intruder.

*Note.* The following section will use condensed notation, due to the equation complexity. The *terminology* is consistent with the rest of the section.

**Space Intersection Rate - Body Volume Intersection:**  $P_T(i_k(x_s, v, \theta, \varphi), c_{i,j,k})$  computation is less straight-forward than other space intersection rates. First let us define the linear intruder  $i_k$  positions  $x$  at time  $t$  (eq. E.8) model, where  $x(t)$  defines intruder position in *avoidance grid euclidean coordinate frame* at time  $t_i$ ,  $v$  defines intruder velocity, and  $t$  is a time offset.

$$x(t) = x_s + v_I.t \quad (\text{E.8})$$

Intruder *horizontal spread*  $\theta$  and *vertical spread*  $\varphi$  are introduced. These spreads represents intruder deviation limits along from linear trajectory prediction  $x(t) \in \mathbb{R}^3$ . The example is given by (fig. E.1) where the intruder starts at point  $x_s$  with fixed velocity  $v$ , the linear trajectory prediction is outlined by blue line. The *predicted intruder position* at time  $t = 10s$  is given by  $x(10)$  (blue point). The ellipsoidal space  $E(x)$  is projected on the plane  $D(x(t))$ . The plane  $D$  (eq. E.9) for point  $x(t)$  and velocity  $v$  is defined as an orthogonal plane to velocity vector  $v \in \mathbb{R}^3$  with origin at intruder position  $x(t)$ .

$$D(x(t), v) = \{a \in \mathbb{R}^3 : (a - x(t)) \perp v, \} \quad (\text{E.9})$$

To construct ellipsoidal space boundary on orthogonal plane  $D(x(t), v)$  some parameters are defined in (eq. E.10). The *scalar distance*  $d_d(x(t))$  is simple Euclidean norm, *maximal horizontal offset*  $d_\theta(x(t))$  is given as product of sinus of horizontal offset angle  $\theta$  and scalar distance  $d_d$ , and *maximal vertical offset*  $d_\varphi(x(t))$  is given a product of sinus of vertical offset angle  $\varphi$  and scalar distance  $d_d$ .

$$\begin{aligned} d_d &= d_d(x(t), x_s) = \|x(t) - x_s\|_2 \\ d_{\theta_{\max}} &= d_\theta(x(t)) = \sin \theta(i_k).d_d(x(t)) \\ d_{\varphi_{\max}} &= d_\varphi(x(t)) = \sin \varphi(i_k).d_d(x(t)) \end{aligned} \quad (\text{E.10})$$

The *Ellipsoid*  $E(x(t), v)$  (eq. E.11) for fixed intruder position  $x(t)$  and fixed intruder velocity  $v$  is given as constrained portion of orthogonal plane  $D(x(t), v)$ . The constraint is defined by an internal coordinate frame  $p \in \mathbb{R}^2$  which is space reduction of plane  $D(x(t), v)$ .

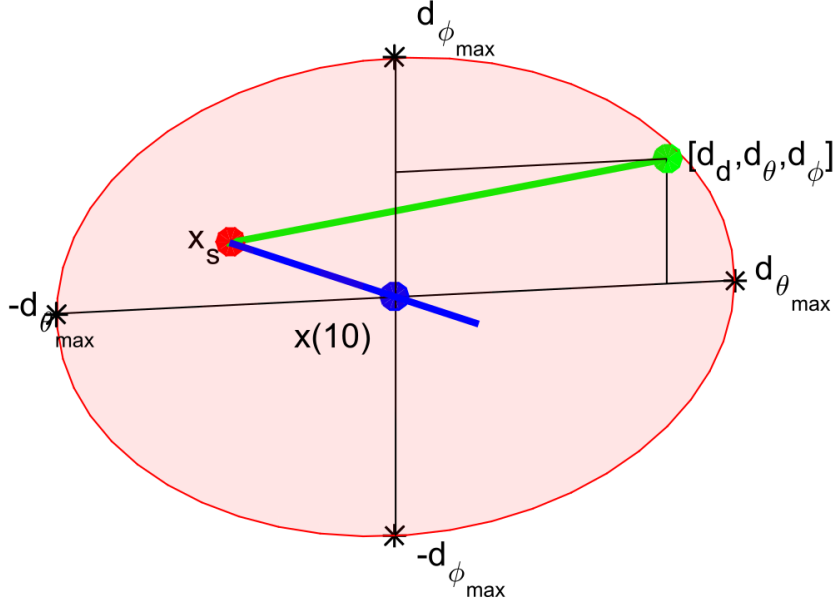


Figure E.1: One rate position  $[d_d, d_\theta, d_\phi]$  (green). deviated from linear trajectory (blue line) at point  $x(10)$ . (blue) with initial position  $x_s$  (red)

The internal coordinate frame  $p \in \mathbb{R}^2$  has origin in  $x(t) \rightarrow \mathbb{R}^2$ . The points of plane  $p$  are bounded by projection  $p = (b - x(t)) \rightarrow \mathbb{R}^2$ , where  $b \in D(x(t), v)$ . The point of ellipsoidal  $p$  is then given as standard ellipse boundary with vertical span  $d_\theta(x(t))$  and horizontal span  $d_\phi(x(t))$ .

The 2D *Ellipsoid*  $E(x(t), v)$  for specific time  $t = 10s$  example is portrayed as red ellipsoid (in fig. E.1).

$$E(x(t), v) = \left\{ b \in \mathbb{R}^3 : b \in D(x(t), v), p = (b - x(t)) \rightarrow \mathbb{R}^2, \left( \frac{p(1)^2}{d_\theta(x(t))^2} + \frac{p(2)^2}{d_\phi(x(t))^2} \right) \leq 1 \right\} \quad (\text{E.11})$$

The expected behavior of an intruder  $i_k$  is to stick to predicted linear trajectory  $x(t)$  (E.8). The probability of deviation should be decreasing with distance from the ellipse center (fig. E.2.).

*Probability density function* for ellipsoid  $E(x(t), v)$  defined in (eq. E.11) is depending on maximal horizontal spread  $d_\theta(x(t))$ , maximal vertical spread  $d_\phi(x(t))$ , defined by (eq. E.10).

Two standard probabilistic distributions are established  $\mathcal{N}(\mu_\theta, \sigma_\theta)$  (eq. E.12) for horizontal spread  $\theta(x(t))$  and  $\mathcal{N}(\mu_\phi, \sigma_\phi)$  (eq. E.13) for vertical spread  $\phi(x(t))$ . The means  $\mu_\theta$  and  $\mu_\phi$  are set to zero, and internal coordinate frame  $p \in \mathbb{R}^2$  where  $x(t) \rightarrow \mathbb{R}^2$  is frame center. The variances  $\sigma_\theta$  and  $\sigma_\phi$  are set as maximal distances on horizontal/vertical spread axes  $d_\theta(x(t))$  and  $d_\phi(x(t))$ .

$$P(x(t), d_\theta) = \mathcal{N}(\mu_\theta, \sigma_\theta) = \mathcal{N}(0, d_\theta(x(t))) \quad (\text{E.12})$$

$$P(x(t), d_\varphi) = \mathcal{N}(\mu_\varphi, \sigma_\varphi) = \mathcal{N}(0, d_\varphi(x(t))) \quad (\text{E.13})$$

The combined *probability density function* for maximal spreads  $d_\theta$  and  $d_\varphi$  is given by (eq. E.14). Because probability density function is defined for internal space  $p \in \mathbb{R}^2$  and one may need to calculate impact rate for cell space  $c_{i,j,k} \in \mathbb{R}^3$ .

The reduction from two parameter probability distribution function to scalar rate distribution function is needed. A scalar rate distribution function  $P(x(t), d_\theta, d_\varphi)$  over ellipsoid  $E(x(t), v)$  is defined as (eq. E.14), where the final rate is given as an average of two partial probabilities.

Final space intersection rate  $P(x(t), d_\theta, d_\varphi)$  needs to be normalized to hold *normal distribution condition* (eq. E.15). Normal distribution condition value (eq. E.15) is given as surface integral over ellipsoid  $E(x(0), v)$  with rate distribution function  $P(x(t), d_\theta, d_\varphi)$ .

$$P(x(t), d_\theta, d_\varphi) = \frac{\mathcal{N}(\mu_\theta, \sigma_\theta) + \mathcal{N}(\mu_\varphi, \sigma_\varphi)}{2} \quad (\text{E.14})$$

$$\iint_{E(x(\tau))} P(x(t), d_\theta, d_\varphi) dd_\theta dd_\varphi = 1 \quad (\text{E.15})$$

Final space intersection rate  $P(x(t), c_{i,j,k}, \theta, \varphi)$  (space portion, time portion is calculated in (eq.??) is given by (eq. E.17). Its mean value of all intersection rates  $P(x(\tau), c_{i,j,k}, \theta, \varphi)$  where  $\tau \in [i_e(c_{i,j,k}), i_l(c_{i,j,k})]$  is fixed point in intersection time interval.

An  $P(x(\tau), c_{i,j,k}, \theta, \varphi)$  (E.16) is integration of rate density function  $P(x(\tau), d_\theta, d_\varphi)$  (eq. E.14) in surface  $E(x(\tau), v)$  to cell  $c_{i,j,k}$  volume intersection.

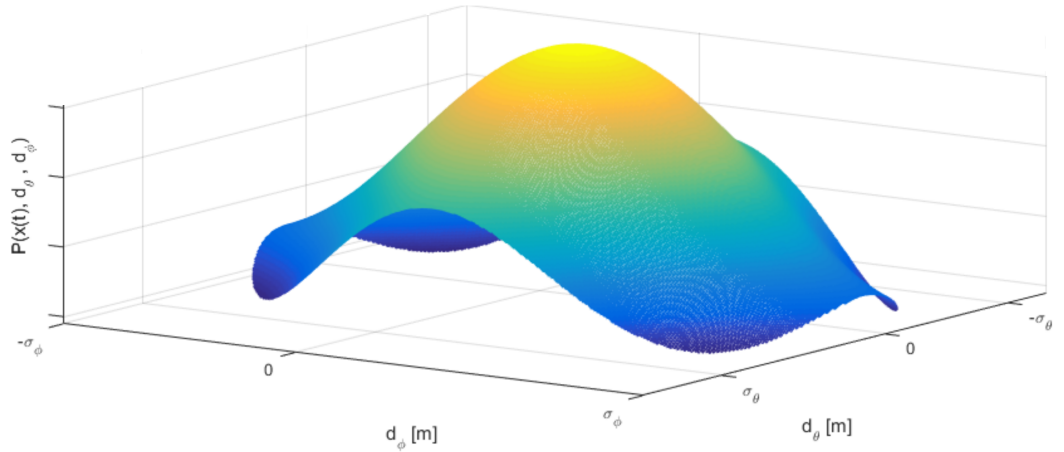


Figure E.2: Probability of intruder  $i_k$  position in ellipsoid  $E(x(t), v)$

To get a volume integration partial rate in surface intersection must be integrated and normalized in time interval  $\tau \in [i_e(c_{i,j,k}), i_l(c_{i,j,k})]$ , the *base intersection probability*  $P_T(i_k(x_s, v, \theta, \varphi), c_{i,j,k})$  is given by (eq. E.17). Example of intersection of intruder  $i_r$  uncertain ellipsoid cone with avoidance grid  $\mathcal{A}(t_i)$  is given in (fig. E.3).

$$P(x(\tau), c_{i,j,k}, \theta, \varphi) = \iint_{E(x(\tau), v) \cap c_{i,j,k}} P(x(\tau), d_\theta, d_\varphi) \quad (\text{E.16})$$

$$P_T(i_k(x_s, v, \theta, \varphi), c_{i,j,k}) = \frac{\int_{i_e(c_{i,j,k})}^{i_l(c_{i,j,k})} P(x(\tau), c_{i,j,k}, \theta, \varphi) d\tau}{i_l(c_{i,j,k}) - i_e(c_{i,j,k})} \quad (\text{E.17})$$

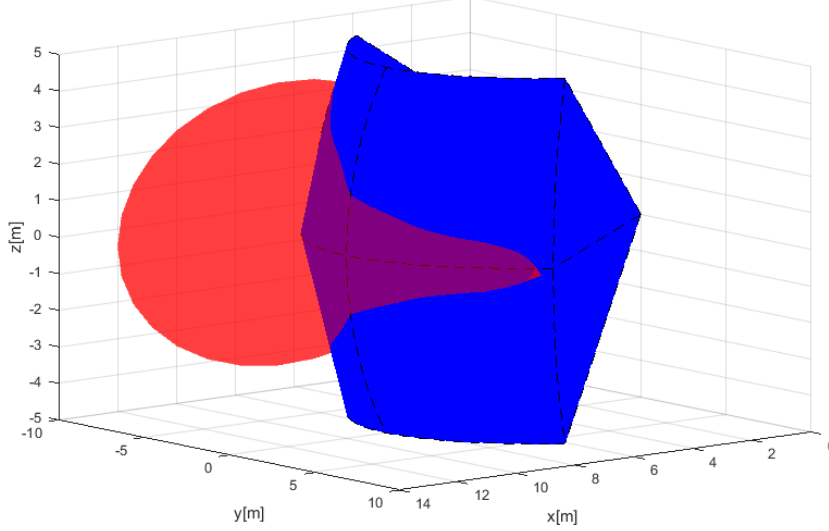


Figure E.3: Avoidance grid  $\mathcal{A}(t_i)$  (blue) intersection with elliptic cone intruder  $i_k(x, v, \theta, \varphi)$  (red) example.

A *numeric approximation* of space intersection rate  $P_T(i_k(x_s, v, \theta, \varphi), c_{i,j,k})$  is more implementation feasible than symbolic calculation due to the multiple intersection constraints and bad intersection algorithm complexity.

Let us define a homogeneous discrete subset of real numbers  $\mathcal{R}$  which is a non-empty subset of real numbers  $\mathbb{R}$ . The set  $\mathcal{R}$  (eq. E.18) is homogeneous that means for an equal interval  $(i, i + 1], i \in \mathbb{Z}$  subset the count of members is equal to some positive natural number  $k$ . The parameter  $k$  can be understood as *unit approximation density*.

Similarly, the power sets  $\mathcal{R}^2 \subset \mathbb{R}^2, \mathcal{R}^3 \subset \mathbb{R}^3, \dots, \mathcal{R}^i \subset \mathbb{R}^i, i \in \mathbb{N}^+$  keeps homogeneous distribution.

$$\mathcal{R} = \left\{ a \in \mathbb{R} : \forall i \in \mathbb{Z}, |i < a \leq i + 1| = k, k \in \mathbb{N}^+, \right. \\ \left. \forall j \in \mathbb{N}^+ a_{j+1} - a_j = m, m \in \mathbb{R}^+ \right\}, \mathcal{R} \subset \mathbb{R} \quad (\text{E.18})$$

The orthogonal plane for  $x(t), v, t \in \mathbb{R}$  is defined by (eq. E.9). The orthogonality property is also kept for any subspace  $\mathcal{R}^n \in \mathbb{R}^n, n \in \mathbb{N}^+$ . Numeric approximation of  $D(x(t), v)$  is given as  $D_D(x(t), v)$  (eq. E.19).

The only difference is that discrete approximation is countable  $|D_D| = m, m \in \mathbb{N}^+$ , but continuous representation  $|D| \approx \infty$  is uncountable. Because ellipsoid is a subset of orthogonal plane it keeps its countability property; therefore  $E_D$  is also countable and

must contain at least one member.

$$D_D(x(t), v) = \{a \in \mathcal{R}^3 : (a - x(t)) \perp v, \}, t \in \mathcal{R} \quad (\text{E.19})$$

The *base ellipsoid*  $E(x(t), v)$  for continuous-space is given by (eq. E.11). Every element, expect the base of internal projection  $\mathcal{R}^2$  and orthogonal plane  $D_D$  is same in discrete case  $E_D(x(t), v)$  (eq. E.20).

$$\bar{E}_D(x(t), v) = \left\{ b \in \mathcal{R}^3 : b \in D_D(x(t), v), p = (b - x(t)) \rightarrow \mathcal{R}^2, \left( \frac{p(1)^2}{d_\theta(x(t))^2} + \frac{p(2)^2}{d_\varphi(x(t))^2} \right) \leq 1 \right\}, t \in \mathcal{R} \quad (\text{E.20})$$

The *numeric calculation disproportion* can occur in case that ellipsoid  $\bar{E}_D(x(t), v)$  (E.20) in case of  $d_\theta(x(t)) \approx 0$  and  $d_\varphi(x(t)) \approx 0$ . The count of ellipsoid members can be  $|\bar{E}_D(x(t), v)| = 0$ , which is in contradiction with assumption  $|\bar{E}_D(x(t), v)| \neq 0$ .

Let assume for discrete times  $\tau = \{t_1, t_2, \dots, t_i\}$ ,  $i \in \mathbb{N}^+$  there exists ellipsoids  $\bar{E}_D(x(t_1), v), \bar{E}_D(x(t_2), v), \dots, \bar{E}_D(x(t_i), v)$  which are non empty and in space  $\mathcal{R}^2$  in internal coordinate frame and space  $\mathcal{R}^3$  in avoidance grid  $\mathcal{A}(t_i)$  coordinate frame. The intersection of these partial ellipsoids in both spaces is equal to:

$$\bar{E}_D(x(t_1), v) \cap \bar{E}_D(x(t_2), v) \cdots \cap \dots \bar{E}_D(x(t_i), v) = \emptyset \quad (\text{E.21})$$

An *empty intersection* enables us to keep homogeneity property of ellipsoids by adding points so it is safe to add specific point  $x(t)$  into empty ellipsoid. But only one, because it does not impact probability density functions  $\mathcal{N}(\mu_\theta, \sigma_\theta)$  and  $\mathcal{N}(\mu_\varphi, \sigma_\varphi)$ , neither space intersection rate density function  $P(x, d_\theta, d_\varphi)$ .

The final ellipsoid used forward  $E_D(x(t), v)$  (eq. E.22) is keeping all properties of ellipsoid  $E(x(t), v)$  (eq. E.22).

$$E_D(x(t), v) = \begin{cases} |\bar{E}_D(x(t), v)| = 0 & : \{x(t)\} \\ |\bar{E}_D(x(t), v)| \geq 0 & : \bar{E}_D(x(t), v) \end{cases} \quad (\text{E.22})$$

The normal distribution condition for rate distribution function  $P_D(x(t), d_\theta, d_\varphi, p)$ , which is instance of to rate density function  $P(x(y), d_\theta, d_\varphi)$  (eq. E.14) is used. This rate distribution must be normalized according to (eq. E.23).

$$\sum_{p \in E_D(x(t))} P_D(x(t), d_\theta, d_\varphi, p) = 1, \forall t \in \mathcal{R}^+ \quad (\text{E.23})$$

The equations for *space intersection rate* are similar to (eq. E.16, E.17). For cell  $c_{i,j,k}$  there exist intruder entry time  $i_e(c_{i,j,k})$  its the earliest intersection with ellipsoid  $E_D(x(i_e(c_{i,j,k}))), v$ . Same situation occurs with intruder leave time  $i_l(c_i, j, k)$ . Because  $E_D$  is countable set, it means additional attributes can be attached to each point  $p \in E_D$ .

Based on system dynamic (eq. ??) the *Time Of Arrival* (TOA) can be calculated. The example of TOA is given in fig. E.4.

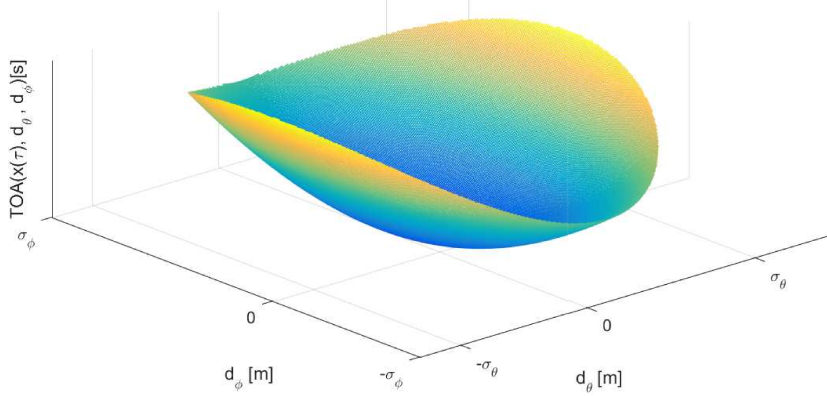


Figure E.4: Time Of Arrival (TOA) for one ellipsoid  $E_D(x(\tau), v)$ .

The intersection rate  $P_D(x(\tau), c_{i,j,k}, \theta, \varphi)$  for one time sample  $\tau$  is given by (eq. E.24), which has similar notation to (eq. E.16), sums are used instead of integrals and discrete rate density function  $P_D(x(\tau), d_\theta, d_\varphi, p)$  for points form ellipse and cell intersection are used as iterator base set  $p \in \{E_D(x(\tau), v) \cap c_{i,j,k}\}$ .

$$P_D(x(\tau), c_{i,j,k}, \theta, \varphi) = \sum_{p \in \{E_D(x(\tau), v) \cap c_{i,j,k}\}} P_D(x(\tau), d_\theta, d_\varphi, p) \quad (\text{E.24})$$

The *space intersection rate*  $P_{TD}(i_k(x_s, v, \theta, \varphi), c_{i,j,k})$  (eq. E.25) is given as mean intersection rate of partial intersections  $P_D(x(\tau), c_{i,j,k}, \theta, \varphi)$  where step set  $T = \{i_e(c_{i,j,k}), \dots, i_l(c_{i,j,k})\}$  contains all viable intersection times with ellipsoids  $E(x(\tau \in T), v)$ . The denominator is basically count of samples in sample time set  $T$ .

$$P_{TD}(i_k(x_s, v, \theta, \varphi), c_{i,j,k}) = \frac{\sum_{\tau=i_e(c_{i,j,k})}^{i_l(c_{i,j,k})} \sum_{p \in E_D(x(\tau), v)} P_D(x(\tau), c_{i,j,k}, \theta, \varphi, p)}{\sum_{\tau=i_l(c_{i,j,k})}^{i_e(c_{i,j,k})} 1} \quad (\text{E.25})$$

An *intersection of intruder cone and cell*  $c_{i,j,k}$  cell is defined by (eq. E.26) The set of point  $p \in \mathcal{R}^3$  where condition of intersection between ellipsoids  $E_D(x(\tau), v)$  for times  $\tau \in \mathcal{R}^+$  and cell space  $c_{i,j,k}$  is met.

$$\mathcal{P}(i_k(x_s, v, \theta, \varphi), c_{i,j,k}) = \bigcup_{\forall \tau \in \mathcal{R}^+} \{p \in \mathcal{R}^3 : p \in c_{i,j,k} \cap E_D(x(\tau), v)\} \quad (\text{E.26})$$

An *intruder time of entry*  $i_e(i_k, c_{i,j,k})$  (eq. E.27), for intruder  $i, k$  and cell  $c_{i,j,k}$  is approximated for discrete point set  $\mathcal{P}(i_k(x_s, v, \theta, \varphi), c_{i,j,k})$  (eq. E.26) as minimal time of arrival  $t_{TOA}(p)$  of member points  $p$ .

$$i_e(i_k, c_{i,j,k}) \approx \min \{t_{TOA}(p) : p \in \mathcal{P}(i_k(x_s, v, \theta, \varphi), c_{i,j,k})\} \quad (\text{E.27})$$



An *intruder time of leave*  $i_l(i_k, c_{i,j,k})$  (eq. E.28), for intruder  $i, k$  and cell  $c_{i,j,k}$  is approximated for discrete point set  $\mathcal{P}(i_k(x_s, v, \theta, \varphi), c_{i,j,k})$  (eq. E.26) as maximal time of arrival  $t_{TOA}(p)$  of member points  $p$ .

$$i_l(i_k, c_{i,j,k}) \approx \max \{t_{TOA}(p) : p \in \mathcal{P}(i_k(x_s, v, \theta, \varphi), c_{i,j,k})\} \quad (\text{E.28})$$

**Combined intersection model:** The *combined intersection model*  $P_{O_I}(i_k, c_{i,j,k}, l, b, s, \tau)$  is defined for intruder  $i_k$  with parameters:

1. *Starting position*  $x_s$  - expected position of intruder  $i_r$  in 3D space at time of avoidance  $t_i$  in avoidance grid frame  $\mathcal{A}(t_i)$ .
2. *Velocity vector*  $v$  - oriented velocity of intruder  $i_r$  at time of avoidance  $t_i$  in avoidance grid frame  $\mathcal{A}(t_i)$ .
3. *Horizontal uncertainty spread*  $\theta$  - defines how much can intruder  $i_r$  deviate on horizontal axis of intruder local coordinate frame (if X+ is the main axis, then Y is horizontal axis in right-hand euclidean coordinate frame), due the properties of intersection definition, the horizontal uncertainty spread can have following values  $\theta \in [0, \pi/2]$ .
4. *Vertical uncertainty spread*  $\varphi$  - defines how much can intruder  $i_r$  deviate on vertical axis of intruder local coordinate frame (if X+ is the main axis in local right-hand euclidean intruder coordinate frame, then Z is horizontal-vertical axis), due to the intersection definition, the vertical uncertainty spread can have following values  $\varphi \in [0, \pi/2]$ .
5. *Body volume radius*  $r$  - defines the body volume of an intruder in meters and it has  $\mathbb{R}^+$  value.

The *flag vector*  $l, b, s, \tau \in \{0, 1\}$  is a parametrization of rate calculation:  $l$  stands for the *lined intersection*,  $b$  stands for *body intersection*,  $s$  stands for the *spread intersection*,  $\tau$  stands for *time account*.

The *space intersection for line*  $P_L(i_k, c_{i,j,k})$  is defined as  $P_T(i_k(x, v), c_{i,j,k})$ , where  $i_k$  is intruder with properties of initial position  $x$ , velocity vector  $v$  and  $c_{i,j,k}$  is target cell. (eq. E.3).

The *space intersection rate for body volume*  $P_B(i_k, c_{i,j,k})$  is defined as  $P_T(i_k(x, v, r), c_{i,j,k})$  (eq. E.7), where intruder  $i_r$  has additional property of the intruder body volume radius  $r$ .

The *space intersection probability for maneuverability uncertainty*  $P_S(i_k, c_{i,j,k})$  is defined as  $P_{TD}(i_k(x_s, v, \theta, \varphi), c_{i,j,k})$  (eq. E.25), where intruder properties  $\theta, \varphi$  stands for intruder horizontal and vertical uncertainty spread.

The *time intersection rate*  $P_{\tau,x}(i_k, c_{i,j,k}) \in [0, 1]$  is defined in (eq. ??). This probability has two calculation modes, first is for 1D intersection (line), second is for volume intersection (body volume, spread elliptic cone).

UAS cell entry time  $t_e$  and cell leave time  $t_l$  time for a vehicle in avoidance grid  $\mathcal{A}(t_i)$  is given by (eq. ??) and (eq. ??).

Intruder leave and entry time for 1D intersections is trivial and is omitted in this section. Intruder entry  $i_e$  and intruder leave  $i_l$  for 3D intersection is given by (eq. E.27, E.28).

All partial rates with respective definition references are summarized in (eq. E.29)

$$\begin{aligned} P_L(i_k, c_{i,j,k}) &= P_T(i_k(x, v), c_{i,j,k}) & (E.3) \\ P_B(i_k, c_{i,j,k}) &= P_T(i_k(x, v, r), c_{i,j,k}) & (E.7) \\ P_S(i_k, c_{i,j,k}) &= P_{TD}(i_k(x_s, v, \theta, \varphi), c_{i,j,k}) & (E.25) \\ P_{\tau,x}(i_k, c_{i,j,k}) &= \frac{\|[i_e(c_{i,j,k}), i_l(c_{i,j,k})] \cap [t_e, t_l]\|}{\|[t_e, t_l]\|} & (??) \end{aligned} \tag{E.29}$$

With definition of all space and time intersection rates (eq. E.29) and given flag vector  $l, b, s, \tau \in \{0, 1\}$  one can formulate combined intersection rate  $P_{OI}(i_k, c_{i,j,k}, l, b, s, \tau)$  (eq. E.30) for intruder  $i_k$  and cell  $c_{i,j,k}$ . The principle is following: *maximum of selected rates product based on flag vector is final intersection rate of intruder  $i_k$  in the cell.*

The time-use flag  $\tau$  is adding time intersection rate  $P_{\tau,x}(i_k, c_{i,j,k})$ , where time intersection rate is defined by  $x = \{L, B, S\}$  for line, body volume, spread ellipse time intersections ( $P_{\tau,L}(i_k, c_{i,j,k}) \neq P_{\tau,B}(i_k, c_{i,j,k}) \neq P_{\tau,S}(i_k, c_{i,j,k})$  for one intruder  $i_k$ ).

$$P_{OI}(i_k, c_{i,j,k}, l, b, s, \tau) = \begin{cases} \tau = 0 & : \max \left\{ \begin{aligned} &P_L(i_k, c_{i,j,k}).l \\ &P_B(i_k, c_{i,j,k}).b \\ &P_S(i_k, c_{i,j,k}).s \end{aligned} \right\} \\ \tau = 1 & : \max \left\{ \begin{aligned} &P_{\tau,L}(i_k, c_{i,j,k}).P_L(i_k, c_{i,j,k}).l \\ &P_{\tau,B}(i_k, c_{i,j,k}).P_B(i_k, c_{i,j,k}).b \\ &P_{\tau,S}(i_k, c_{i,j,k}).P_S(i_k, c_{i,j,k}).s \end{aligned} \right\} \end{cases} \tag{E.30}$$

# Bibliography